A system of hidden quantum dots in the magnetic field: a near-field approach

2004 J. Phys.: Condens. Matter 16 543

(http://iopscience.iop.org/0953-8984/16/4/003)

INSTITUTE OF PHYSICS PUBLISHING JOURNAL OF PHYSICS: CONDENSED MATTER

J. Phys.: Condens. Matter **16** (2004) 543–552 PII: S0953-8984(04)70774-2

A system of hidden quantum dots in the magnetic field: a near-field approach

Yu Demidenko[1], **A Kuzyk**[2,3], **V Lozovski**[2] **and O Tretyak**[2]

[1] Institute of Semiconductor Physics, National Academy of Sciences of Ukraine, Nauki avenue 45, 03028, Kyiv, Ukraine
[2] Radiophysical Faculty of National Taras Shevchenko Kyiv University, Glushkov avenue 2, Building 5, 03022, Kyiv, Ukraine

E-mail: Anthony_k@ukr.net

Received 17 October 2003
Published 16 January 2004
Online at stacks.iop.org/JPhysCM/16/543 (DOI: 10.1088/0953-8984/16/4/003)

Abstract

The influence of an interface on the energy level structure of hidden quantum dots was studied. A self-consistent formalism was used for the calculation of the linear response of a single hidden quantum dot and a dilute layer of quantum dots in the presence of a static homogenous magnetic field. The article studies how the shifts of energy levels caused by self-field interactions (the so-called Lamb shifts) depend on the distance to the surface and magnetic field. Numerical calculations show that the interaction between the quantum dot and the surface leads to substantial Lamb shifts. These shifts can reach relative values of more than 10%, and strongly decrease if the distance between the quantum dot and the surface increases. The influence of a concentration of quantum dots in a hidden layer was studied, and absorption spectra were calculated. The numerical calculations show that the influence of interaction between the quantum dots inside a dilute layer on the absorption profile is rather weak.

(Some figures in this article are in colour only in the electronic version)

1. Introduction

Nowadays there is great interest in the electromagnetic properties of nano-systems (systems that contain particles with linear dimensions of about 1–100 nm). These systems have some interesting electron and optical properties [1–4]. Some of the most fascinating nano-systems are quantum dots (QDs). Owing to the electron confinement QDs represent the extreme case, since the motion of electrons and holes is localized in all directions in these systems and the electronic structure is discrete [5]. QDs are microstructures in which the extent of the electronic wavefunction is comparable with the effective Bohr radius but still far larger than

[3] Address for correspondence: Lomonosov street 35 /504, 03022 Kyiv, Ukraine.

the size of single atoms. In contrast to the real atoms, in which the potential is determined by the Coulomb interaction, the experiments performed on field-effect-confined QDs show that good agreement between measurements and theory is achieved assuming the QD potential is parabolic [6, 7]. Indeed, any physical potential will deviate from the strictly parabolic one, especially near the edge of the potential. However, any smooth physical potential is expected to be adequately described by a simple parabolic model. This is an obvious advantage because in this case the Schrödinger equation can be solved relatively easily.

Very often QDs are situated close to the surface (see for example [8, 9]). The fabrication and experimental studying of a single QD is a very difficult problem, and as a rule people deal with QD arrays [10, 11]. Because the QD is not a point-like object, the local-field effects have to be taken into account in order to describe the electrodynamics of such systems [12, 13]. The local-field effects without magnetic field in a single QD in a homogeneous medium were studied in [14, 15] and the influence of the surface was described in [16]. Recently, spin-dependent phenomena have been studied with respect to the development of so-called spintronics [17, 18], which is based on the effects caused by the injection of spin polarized carriers. Owing to this, studies of nanostructures in the presence of magnetic field have become very active [19–21]. Then, in [21] the luminescence of InAs/Ga/As and InGaAs/GaAs QDs covered by 50 nm and 300 nm films was measured under a magnetic field up to 10 T. A small shift ($\leqslant 100\ \mu$eV) of the luminescence peak was found at the 10 T magnetic field. The present work is to a large extent based on [22], in which the calculation of the effective polarizability for a particle situated in a homogeneous medium with the presence of a magnetic field was made.

The purpose of this paper is to present a self-consistent formalism for the calculation of the linear response (effective polarizability) of a single QD and a dilute layer of QDs under the surface of a solid in the presence of a static homogenous magnetic field, and to make the theoretical prediction of the absorption spectra. The interface in the system leads to the appearance of an additional part of the local-field caused by the interaction between the particle and the surface. This local-field and magnetic field induce some reconstruction of energy levels of the QD system. It has been shown that interactions between the particle and the surface determine the electrodynamical properties of the system [16]. A detailed description of the local-field effect and a self-consistent formalism are given in review [12].

Thus, the influence of the surface and external magnetic field on the energy level structure of a hidden quantum dot is the main problem of this work.

2. Energy level structure

Let the quantum dot be located under the surface of the solid and the external magnetic field act on the system (see, figure 1(a)). As is well known, the lowest excited state level of the conduction band of a single isotropic parabolic QD under the action of external magnetic field splits into three states. If the magnetic field is taken to be along the z direction ($\vec{B} = B\vec{e}_z$) and the circular gauge $\vec{A} = B(-y/2, x/2, 0)$ is used, then the total Hamiltonian can be written as

$$H = -\frac{\hbar^2}{2m_\mathrm{e}}\nabla^2 - \frac{\mathrm{i}}{2}\hbar\omega_\mathrm{c}\left(x\frac{\partial}{\partial y} - y\frac{\partial}{\partial x}\right) + \frac{1}{2}m_\mathrm{e}\omega_\perp^2(x^2+y^2) + \frac{1}{2}m_\mathrm{e}\omega_0^2 z^2, \quad (1)$$

where ω_0 is the parabola frequency, $\omega_\mathrm{c} = eB/m_\mathrm{e}$ is the so-called cyclotron frequency, and $\omega_\perp = (\omega_0^2 + \omega_\mathrm{c}^2/4)^{1/2}$. Moreover, m_e and e denote the effective mass and the charge of the electron, respectively. The Hamiltonian (equation (1)) can be solved easily enough by the introduction of cylindrical coordinates ($x = r_\perp\cos\varphi$, $y = r_\perp\sin\varphi$, $z = r_\parallel$). The wavefunctions corresponding to this Hamiltonian have the form

$$\psi_{\lambda\mu\nu}(\vec{R}) = a_{\lambda\mu\nu}H_\lambda(\beta_\parallel R_\parallel)R_\perp^{|\mu|}L_\nu^{|\mu|}(\beta_\perp^2 R_\perp^2)\exp[-\tfrac{1}{2}(\beta_\perp^2 R_\perp^2 + \beta_\parallel^2 R_\parallel^2) + \mathrm{i}\mu\varphi]. \quad (2)$$

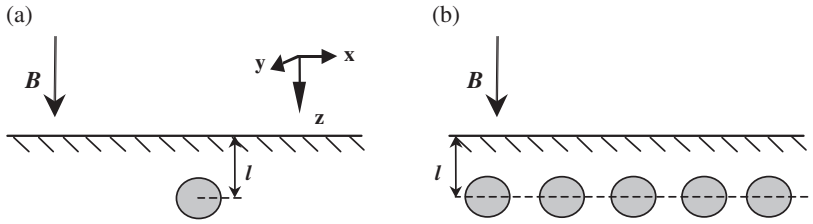

Figure 1. A sketch of the system investigated with a single QD (a) and a layer of QDs (b) located under a surface of a solid.

Here $a_{\lambda\mu\nu}$ is the normalization constant, $\beta_\parallel = (m_e\omega_0/\hbar)^{1/2}$, and $\beta_| = (m_e\omega_\perp/\hbar)^{1/2}$. In equation (2), H_λ and $L_\nu^{|\mu|}$ are Hermite and Laguerre polynomials respectively. Following [22], this work takes into consideration only the ground state $|000\rangle$ and next three lowest-lying states $|100\rangle, |0\bar{1}0\rangle, |010\rangle$ with energies relative to the ground state of $E_0 = \hbar\omega_0$, $E_- = \hbar\omega_\perp - 1/2\hbar\omega_c$, and $E_+ = \hbar\omega_\perp + 1/2\hbar\omega_c$. For convenience, the states were relabelled according to $|0\rangle = |000\rangle, |+\rangle = |010\rangle, |-\rangle = |0\bar{1}0\rangle$ and $|z\rangle = |100\rangle$. The transition current densities for the transitions from $|0\rangle$ to $|-\rangle, |+\rangle, |z\rangle$ are denoted here as $\vec{j}_0^-(\vec{R})$, $\vec{j}_0^+(\vec{R})$, and $\vec{j}_0^z(\vec{R})$, respectively. It is found that

$$\vec{j}_0^z(\vec{R}) = \frac{e\hbar}{\sqrt{2}\mathrm{i}m_e}\frac{\beta_\parallel^2\beta_\perp^2}{\pi^{3/2}}\exp(-\beta_\perp^2R_\perp^2 - \beta_\parallel^2R_\parallel^2)\vec{e}_z, \tag{3}$$

$$\vec{j}_0^\pm(\vec{R}) = \frac{e\hbar}{\sqrt{2}\mathrm{i}m_e}\frac{\beta_\parallel\beta_\perp^3}{\pi^{3/2}}\exp(-\beta_\perp^2R_\perp^2 - \beta_\parallel^2R_\parallel^2)\vec{e}_\pm. \tag{4}$$

3. The effective polarizability

Further calculations are to a large extent based on [22]. However, for the convenience of readers we present them here. The effective polarizability can be defined as the function connecting the induced dipole momentum $\vec{p}(\omega)$ and the background field $\vec{E}^{(0)}(0)$ in the centre of the QD:

$$\vec{p}(\omega) = \overleftrightarrow{\alpha}(\omega)\vec{E}^{(0)}(0). \tag{5}$$

In general the dipole momentum can be calculated as

$$\vec{p}(\omega) = \frac{\mathrm{i}}{\omega}\int_V \vec{j}(\vec{R})\,\mathrm{d}\vec{R}, \tag{6}$$

where integration is over the volume V of the QD. The spatial current density $\vec{j}(\vec{R})$ is

$$\vec{j}(\vec{R}) = \int_V \mathrm{d}^3R'\overleftrightarrow{\sigma}(\vec{R},\vec{R}')\vec{E}(\vec{R}'). \tag{7}$$

The expression (6) can be written in the form

$$\vec{p}(\omega) = \frac{\mathrm{i}}{\omega}\int_V \vec{j}(\vec{R})\,\mathrm{d}\vec{R} = \frac{\mathrm{i}}{\omega}\int_V\int_V \overleftrightarrow{\sigma}(\vec{R},\vec{R}')\vec{E}\,\mathrm{d}^3R'\,\mathrm{d}^3R. \tag{8}$$

In equations (7) and (8), $\overleftrightarrow{\sigma}(\vec{R},\vec{R}')$ is the nonlocal conductivity tensor, which at low temperature is given by

$$\overleftrightarrow{\sigma}(\vec{R},\vec{R}') = \frac{\mathrm{i}}{\omega}\sum_n\left[\frac{1}{\hbar(\omega+\mathrm{i}\nu)+E_0-E_n}\vec{j}_n^0(\vec{R})\vec{j}_0^n(\vec{R}') - \frac{1}{\hbar(\omega+\mathrm{i}\nu)-E_0+E_n}\vec{j}_0^n(\vec{R})\vec{j}_n^0(\vec{R}')\right], \tag{9}$$

where $n = \{+, -, z\}$, and ν is the decay constant. This equation can be reduced to the form

$$\overleftrightarrow{\sigma}(\vec{R}, \vec{R}') = \frac{-\mathrm{i}}{\hbar\omega}[a_+(\omega)\vec{j}_0^+(\vec{R})\vec{j}_0^-(\vec{R}') + a_-(\omega)\vec{j}_0^-(\vec{R})\vec{j}_0^+(\vec{R}') + a_z(\omega)\vec{j}_0^z(\vec{R})\vec{j}_0^z(\vec{R}')], \tag{10}$$

with

$$a_\pm = \frac{2\omega_\pm}{(\omega + \mathrm{i}\nu)^2 - \omega_\pm^2}, \qquad a_z = \frac{2\omega_0}{(\omega + \mathrm{i}\nu)^2 - \omega_0^2}, \qquad \omega_\pm = \omega_\perp \pm \frac{1}{2}\omega_\mathrm{c}. \tag{11}$$

When combined, equations (8) and (10) yield

$$\vec{p}(\omega) = \frac{1}{\hbar\omega^2}[a_+(\omega)\vec{J}_0^+\gamma_- + a_-(\omega)\vec{J}_0^-\gamma_+ + a_z(\omega)\vec{J}_0^z\gamma_z], \tag{12}$$

where

$$\vec{J}_0^n = \int_V \vec{j}_0^n(\vec{R})\,\mathrm{d}^3R \qquad \text{and} \qquad \gamma_n = \int_V \vec{E}(\vec{R})\vec{j}_0^n(\vec{R})\,\mathrm{d}^3R.$$

For the calculation of the unknown numbers γ_n, one needs to know the electrical field inside the particle. For this purpose the self-consistent equation of Lippmann–Shwinger is used:

$$\vec{E}(\vec{R}) = \vec{E}^{(0)}(\vec{R}) - \mathrm{i}\frac{\mu_0}{\hbar}\sum_n a_n \int_V \mathrm{d}^3R'\overleftrightarrow{G}(\vec{R}, \vec{R}')\vec{j}_0^n(\vec{R}') \int_V \mathrm{d}^3R\,\vec{j}_0^n(\vec{R})\vec{E}(\vec{R}). \tag{13}$$

Here $\overleftrightarrow{G}(\vec{R}, \vec{R}')$ is a Green function (the photon propagator) consisting of two parts [12, 13] (in contrast to [22] where the Green function has only a direct part).

$$\overleftrightarrow{G}(\vec{R}, \vec{R}') = \overleftrightarrow{D}(\vec{R}, \vec{R}') + \overleftrightarrow{I}(\vec{R}, \vec{R}'). \tag{14}$$

Here $\overleftrightarrow{D}(\vec{R}, \vec{R}')$ is the direct part of the Green function that corresponds to the infinite space, and $\overleftrightarrow{I}(\vec{R}, \vec{R}')$ is the indirect part of the Green function that describes the interactions with the surface. Because the linear dimension of the quantum dots and the distances between quantum dots and the surface are much less than the wavelength of the external field, the so-called near-field approximation [12] can be used. The direct part of the Green function in the near-field approximation can be written as

$$\overleftrightarrow{D}(\vec{R}, \vec{R}') = \frac{1}{4\pi}\left[\frac{c^2}{\omega^2 \cdot R^3}\overleftrightarrow{U} - \frac{3c^2}{\omega^2 \cdot R^3}\vec{e}_R\vec{e}_R\right], \tag{15}$$

with $\overleftrightarrow{U}$ being a unit dyadic, $R = |\vec{R} - \vec{R}'|$ and $\vec{e}_R = \vec{R}/R$. The indirect part of the photon propagator in this approximation is

$$\overleftrightarrow{I}(\vec{R}, \vec{R}') = \overleftrightarrow{D}(\vec{R}, \vec{R}'_M) \cdot \overleftrightarrow{M}, \tag{16}$$

where

$$\overleftrightarrow{M} = -\frac{\varepsilon - 1}{\varepsilon + 1}\begin{pmatrix} 1 & 0 & 0 \\ 0 & 1 & 0 \\ 0 & 0 & -1 \end{pmatrix} \tag{17}$$

and $\vec{R}'_M = (x', y', -z')$. In equation (17) ε means the dielectric constant of the medium in which the quantum dots are embedded. Then the Lippmann–Shwinger equation (13) can be reduced to a system of linear equations [15]

$$\gamma_m = \gamma_m^0 - \sum_n a_n N_n^m \gamma_n, \tag{18}$$

and the unknown numbers γ_n can be found. Here the near-field approximation is used:

$$\gamma_m^0 = \int_V \mathrm{d}^3 R\, \vec{E}^{(0)}(\vec{R})\vec{j}_0^m(\vec{R}) \cong \int_V \mathrm{d}^3 R'\, \vec{j}_0^m(\vec{R}') \cdot \vec{E}^{(0)}(0) \equiv \vec{J}_0^m \vec{E}^{(0)}(0) \tag{19}$$

$$N_n^m = \frac{\mu_0}{\hbar} \int \int_V \mathrm{d}^3 R\, \mathrm{d}^3 R'\, \vec{j}_0^n(\vec{R}) \overleftrightarrow{G}(\vec{R}, \vec{R}') \vec{j}_0^m(\vec{R}'). \tag{20}$$

As the result the dipole momentum can be written in the form

$$\vec{p}(\omega) = \overleftrightarrow{\alpha}(\omega)\vec{E}^{(0)}(0),$$

where

$$\overleftrightarrow{\alpha}(\omega) = -\frac{e^2\hbar}{2\mathrm{i}\omega m_\mathrm{e}^2}\left[\frac{a_+(\omega)\beta_\perp^2}{1 + a_+(\omega)N_-^+}\vec{e}_+\vec{e}_- + \frac{a_-(\omega)\beta_\perp^2}{1 + a_-(\omega)N_+^-}\vec{e}_-\vec{e}_+ + \frac{a_z(\omega)\beta_\parallel^2}{1 + a_z(\omega)N_{zz}}\vec{e}_z\vec{e}_z\right]. \tag{21}$$

From equation (21) it is seen that N_n^m determines the shifts (the so-called Lamb shifts) and the spontaneous decay rates of the energy levels [15]. Thus, N_-^+ for $\omega = (E_+ - E_0)/\hbar$ determines the shift of the $|0\rangle \to |+\rangle$ transition, N_+^- for $\omega = (E_- - E_0)/\hbar$ determines the shift of the $|0\rangle \to |-\rangle$ transition and N_z^z for $\omega = (E_z - E_0)/\hbar$ determines the shift of the $|0\rangle \to |z\rangle$ transition.

Let the dilute layer of QDs be hidden under the surface (figure 2(b)). We define the dilute layer as a layer in which the distance between neighbouring particles is rather long. This means that the electrodynamical properties of the particles are mainly formed by the interaction between the particle and the surface. As was shown in previous works [23–25], for an evenly distributed layer of quantum dots, the effective polarizability of the dilute layer of QDs can be written in the form

$$\overleftrightarrow{\alpha}_{\mathrm{array}}(\omega, l) = [\overleftrightarrow{\alpha}(\omega, l)^{-1} - n\overleftrightarrow{G}^{(T)}(\vec{k}, \omega, l)]^{-1}, \tag{22}$$

where $\overleftrightarrow{\alpha}(\omega, l)$ is the effective polarizability of the single QD, n is the concentration of QDs in the layer, l is the distance to the surface, and $\overleftrightarrow{G}^{(T)}(\vec{k}, \omega, l)$ is the total Green function of two semi-spaces with a flat interface written in k–z representation [13] with $z = z' = l$. The total Green function describes all contributions (near-field, middle-field, and far-field) of electrodynamical interactions. The calculation of the total Green function can be found in [26].

It is necessary to stress once more than the physical meaning of the influence of a surface on the quantum dot energy characteristics is caused by strong inhomogeneities of the local field near the interface. The stronger the inhomogeneities the larger the energy levels shifts. In connection with this statement it is natural to expect that the decrease of the distance from a particle to the interface will increase the local field effects; in other words, the Lamb value shifts.

4. Numerical results and discussion

The numerical calculations were made for a GaAs quantum dot with $\hbar\omega_0 = 7.5$ meV, $\nu = 0.01\omega_0$ and radius of 20 nm located under the surface in an AlGaAs medium. The single-particle shifts can be calculated from equation (20). The calculation of dependences of line shifts on the distance l between the QD and a surface shows that Lamb shifts decrease when l increases. Moreover, the analytical evaluations provide the dependence on l as l^{-3}. This is a consequence of the near-field interaction between the QD and a surface when l is rather small. It should be pointed out that the shifts are indeed perceptible. Namely, at $l = 20$ nm the shifts ΔE are: for the $|0\rangle \to |-\rangle$ transition $\Delta E \approx 2.75$ meV; for the $|0\rangle \to |z\rangle$ transition $\Delta E \approx 2.15$ meV; for the $|0\rangle \to |+\rangle$ transition $\Delta E \approx 1.75$ meV. Increasing the distance l up to

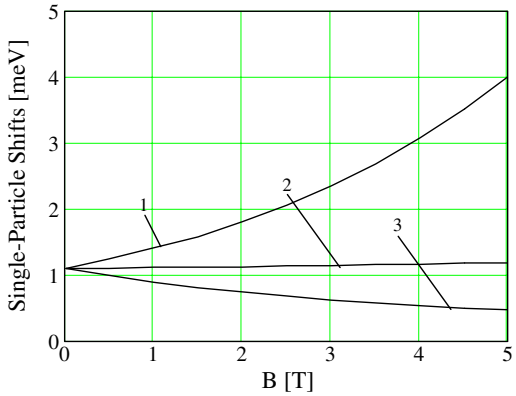

Figure 2. Single-particle shifts as a function of the magnetic field strength. Curve 1 corresponds to the $|0\rangle \to |-\rangle$ transition; curve 2 corresponds to the $|0\rangle \to |z\rangle$ transition; curve 3 corresponds to the $|0\rangle \to |+\rangle$ transition. The distance between the surface and the particle is $l = 25$ nm.

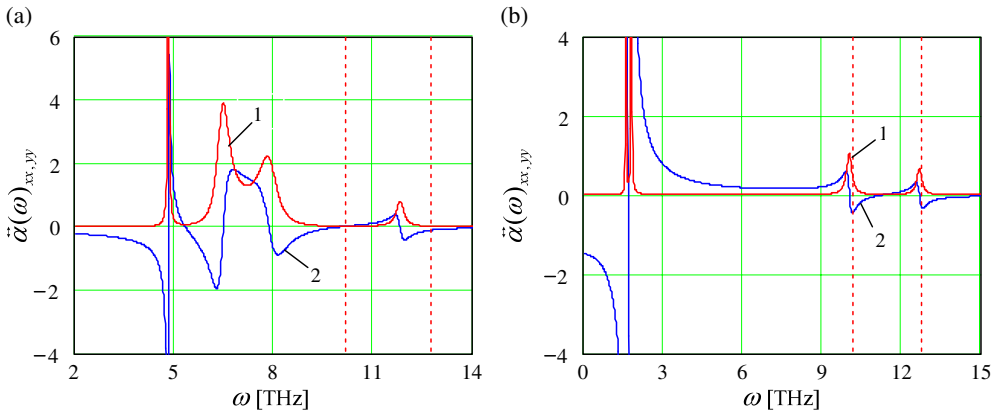

Figure 3. The xx- and yy-components ($\overleftrightarrow{\alpha}(\omega)_{xx,yy}$) of the effective polarizability (arbitrary units) as functions of frequency. The distances to the surface are $l = 30$ nm (a), $l = 60$ nm (b). The magnetic field strength $B = 1$ T. Curve 1 indicates the imaginary part and curve 2 indicates the real part. Vertical dashed lines correspond to the values $\frac{E_-}{\hbar}$ (left) and $\frac{E_+}{\hbar}$ (right).

40 nm leads to decreasing shifts. The shifts become less than 0.5 meV. Thus, the relative values of the shifts can be larger than 10% for a QD located very close to the surface. The shifts, in contrast, are less than 0.01% for the GaAs QD with the same parabolic frequency situated in a homogeneous medium [22]. Therefore it is extremely important for the proper consideration of a hidden QD and QD layers to keep in mind the possibility of the influence of the surface. The influences of magnetic field on the Lamb shifts are illustrated in figure 2. Clearly the transitions $|0\rangle \to |-\rangle$ and $|0\rangle \to |+\rangle$, i.e., those involving a change of the magnetic quantum number, are mostly influenced by the magnetic field. The character of the dependences of the shifts on the magnetic field is the same as in [22]. All the resonance conditions of the system are determined by the components of the effective polarizability tensor. For a single QD, spectral dependences can be calculated from (21), and numerical results are illustrated in figures 3 and 4. As is seen, the resonance frequencies asymptotically approach the values $E_-/\hbar$, $E_+/\hbar$ and $E_0/\hbar$ (compare figure 3(a) with 3(b) and 4(a) with 4(b)).

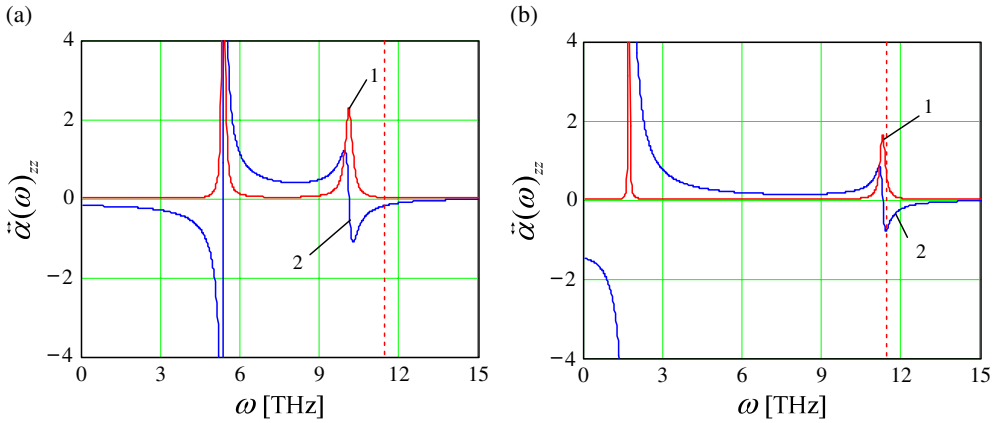

Figure 4. The zz- component ($\overleftrightarrow{\alpha}(\omega)_{zz}$) of the effective polarizability (arbitrary units) as a function of frequency. The distances to the surface are $l = 30$ nm (a), $l = 60$ nm (b). The magnetic field strength $B = 1$ T. Curve 1 indicates the imaginary part and curve 2 indicates the real part. The vertical dashed line corresponds to the value $\frac{E_0}{\hbar}$.

Let us compare figures 3(a) and (b) which demonstrate the influence of the surface on the Lamb shifts of the lines characterized by the transitions $|0\rangle \rightarrow |\pm\rangle$. The appreciable shifts at distance $l = 30$ nm vanish at $l = 60$ nm. A similar effect is demonstrated for the transition $|0\rangle \rightarrow |z\rangle$ (see figures 4(a) and (b)). This fact can be easily understood if we take into consideration the near-field regime in which the electrodynamical interaction is quasi-static. Then, the dependence of the single-particle Lamb shift on the distance between the QD and the surface is proportional to l^{-3}. It should be emphasized that a profile of the line corresponding to the transition $|0\rangle \rightarrow |-\rangle$ at small distances l does not only shift but also split (there are three maxima in figure 3(a)). This means that the local-field effect in surface-particle interaction is most effectively disclosed for the transition characterized by the lowest energy. Indeed, a decrease of the distance l leads to the closing together of the split peaks. Then, at $l = 60$ nm (figure 3(b)) the splitting is not observed (two maxima).

The spectral dependence of the components for a dilute layer of QDs can be calculated using equation (22). The spectral behavior of the imaginary parts of the $\overleftrightarrow{\alpha}_{\text{array}}(\omega, l)$ diagonal components (figure 5) is the most interesting because in addition to the resonance conditions they determine the absorption spectra of the layer (for absorption spectra of QDs see also [27, 28]). As can be seen, for a concentration 10^{14} m^{-2}, the relative change of the magnitude of the absorption peaks of $\overleftrightarrow{\alpha}_{\text{array}}(\omega, l)_{xx}$ and $\overleftrightarrow{\alpha}_{\text{array}}(\omega, l)_{yy}$ is about 1%. In contrast, the relative change of the absorption peak of $\overleftrightarrow{\alpha}_{\text{array}}(\omega, l)_{zz}$ is about 10%. So the lateral interactions (between the dots) mostly influence the transitions $|0\rangle \rightarrow |z\rangle$. This can be explained by the method of a mirror, which states that the interactions between two dipoles that are normal to surface is larger than the interaction between two dipoles parallel to the surface. The change of the components of the polarizability tensor and eventually the absorption spectra profile is almost negligible for concentrations of QDs in the layer less than 10^{13} m^{-2}. The lateral interactions between molecules characterized by very strong polarizability, in contrast, can lead to broadening and splitting of the line, as was shown earlier [23]. It is convenient to consider the absorption spectra in terms of s- and p-polarized waves. For a p-polarized wave the intensity of absorption

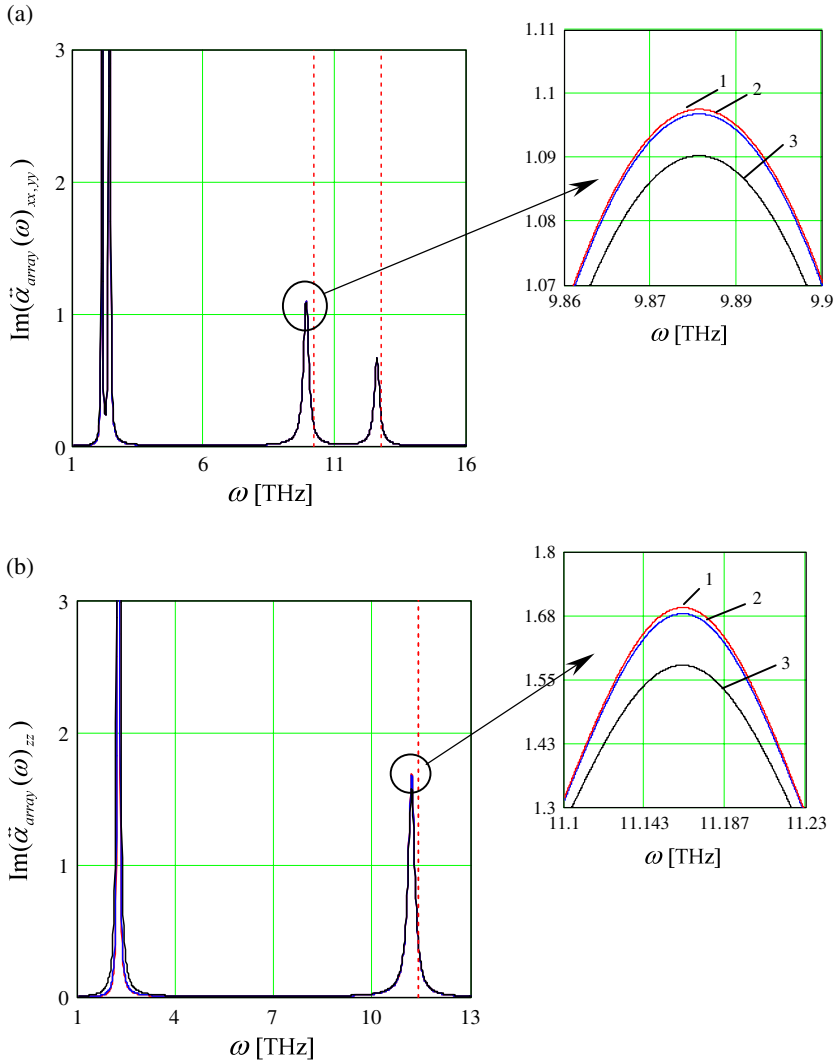

Figure 5. The imaginary parts of the diagonal components ($\overleftrightarrow{\alpha}_{\mathrm{array}}(\omega)_{xx,yy}$ (a), $\overleftrightarrow{\alpha}_{\mathrm{array}}(\omega)_{zz}$ (b)) of the effective polarizability tensor of a QD array (arbitrary units) as functions of frequency for different values of concentration. The distance to the surface $l = 50$ nm; the magnetic field strength $B = 1$ T. Curve 1 corresponds to the concentration $n = 0$ m^{-2} (the case of a single QD); curve 2 corresponds to the concentration $n = 10^{13}$ m^{-2}; curve 3 corresponds to the concentration $n = 10^{14}$ m^{-2}. The vertical dashed lines indicate the values $E_-/\hbar$ and $cE_+/\hbar$ (a), and $E_0/\hbar$ (b).

$$I(\omega,\theta)_{\mathrm{p}} \propto \mathrm{Im}[\overleftrightarrow{\alpha}_{\mathrm{array}}(\omega)_{xx}\cos^2(\theta) + \overleftrightarrow{\alpha}_{\mathrm{array}}(\omega)_{zz}\sin^2(\theta) + \overleftrightarrow{\alpha}_{\mathrm{array}}(\omega)_{zx}\sin(\theta)\cos(\theta) + \overleftrightarrow{\alpha}_{\mathrm{array}}(\omega)_{xz}\sin(\theta)\cos(\theta)]. \tag{23}$$

For an s-polarized wave

$$I(\omega,\theta)_s \propto \mathrm{Im}[\overleftrightarrow{\alpha}_{\mathrm{array}}(\omega)_{yy}]. \tag{24}$$

The absorption spectrum of a p-polarized wave has three resonance frequencies (figure 6(a)). The absorption spectrum of an s-polarized wave, in contrast, has only two peaks (figure 6(b)), due to the directions of the transition currents (3, 4). In addition, the spectra of a p-polarized

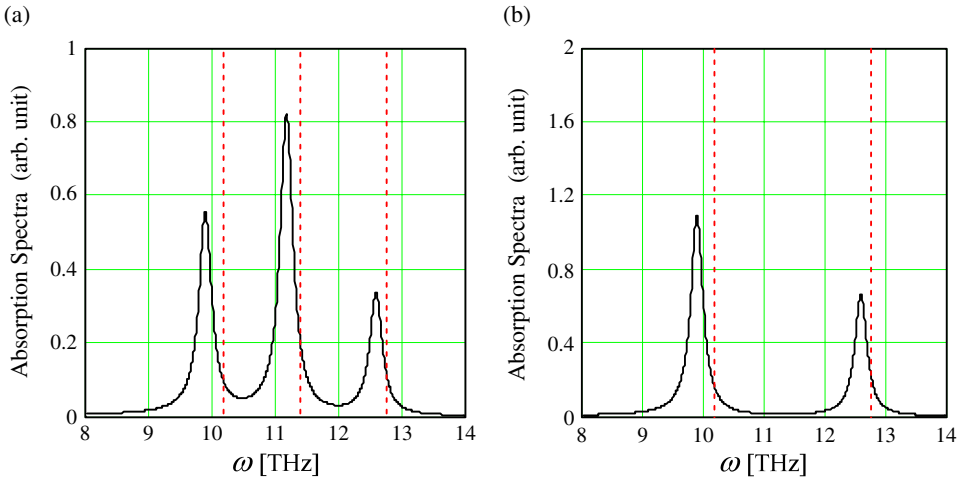

Figure 6. The absorption spectra for p- (a) and s-polarized (b) waves. The distance to the surface $l = 50$ nm; the magnetic field strength $B = 1$ T; concentration $n = 10^{14}$ m^{-2}. The vertical dashed lines indicate the values $E_-/\hbar$, $cE_0/\hbar$ and $E_+/\hbar$ (a), and $E_-/\hbar$ and $cE_+/\hbar$ (b). In (a) the incidence angle $\theta = \pi/3$.

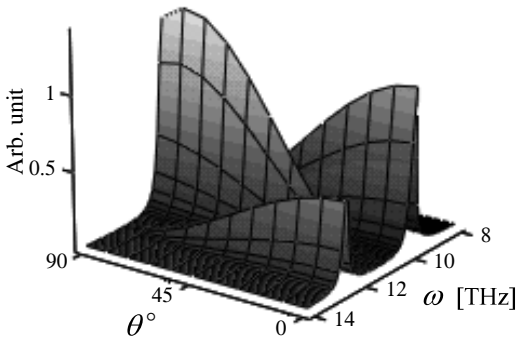

Figure 7. The absorption spectra of a p-polarized wave as a function of the incidence angle θ (in deg).

wave depend on the incidence angle of the wave (figure 7). A wave with angle $\pi/2$ induces $|0\rangle \to |z\rangle$ transitions, while a wave with angle 0 induces $|0\rangle \to |-\rangle$ and $|0\rangle \to |+\rangle$ transitions. The spectrum of an s-polarized wave does not depend on the incidence angle. Then, the absorption of an s-polarized field is defined by transitions $|0\rangle \to |\pm\rangle$. But the absorption of a p-polarized field depends on all considered transitions $|0\rangle \to |\pm\rangle$ and $|0\rangle \to |z\rangle$. As a result, a standard set of the Zeeman triplet can be seen in figure 6(a).

Finally it should be noted that the parameters of the GaAs system QD in the AlGaAs substrate used here ($\hbar\omega_0 = 7.5$ meV, $\nu = 0.01\omega_0$) were chosen here only for determination. Using other parameters gives us obviously similar (at least qualitatively) results.

5. Summary

We applied a self-consistent approach to investigate the local-field effects in a single QD and a dilute layer of QDs hidden under the surface in the presence of a magnetic field. The single QD

is assumed to have parabolic and isotropic potential. For a single QD the effective polarizability was calculated. The analysis demonstrates that only transitions involving a change of the magnetic quantum number are significantly influenced by the magnetic field. It is shown that in contrast to the case of a homogeneous medium, the shifts can be significant in the presence of the surface. The effective polarizability was calculated for the dilute layer. Numerical analysis of the influence of the lateral interactions on the absorption profile has shown that this influence is rather weak. This means that lateral interactions can be neglected at concentrations of QD layer lower than 10^{13} m^{-2}. Then often the QD array can be treated as a single QD $\times$ concentration. However, the predicted effects for the considered concentrations are within experimental reach. It should be noted that the magnetic field could be effective for control of the energy structure of the QD systems.

References

[1] Bastard G 1988 *Wave Mechanics Applied to Semiconductor Heterostructures* (New York: Halsted Press)
[2] Weisbuch C and Vinter B 1991 *Quantum Semiconductor Structures: Fundamentals and Applications* (Boston, MA: Academic)
[3] Mitin V V, Kochelap V A and Stroscio M A 1999 *Quantum Heterostructures* (Cambridge: Cambridge University Press)
[4] Vasko F T and Kuznetsov A V 1999 *Electronic States and Optical Transitions in Semiconductor Heterostructures* (New York: Springer)
[5] Reimann S M and Manninen M 2002 *Rev. Mod. Phys.* **74** 1283
[6] Demel T, Heitmann D, Grambow P and Ploog K 1990 *Phys. Rev. Lett.* **64** 788
[7] Burkard G, Loss D and DiVincenzo D P 1999 *Phys. Rev.* B **59** 2070
[8] Hess H F, Betzig E, Harris T D, Pfeifer L N and West K W 1994 *Science* **264** 1740
[9] Obermüller C *et al* 1999 *Appl. Phys. Lett.* **74** 3200
[10] Kops U, Blome P G, Wenderoth M, Ulbrich R G, Geng C and Scholz F 2000 *Phys. Rev.* B **61** 1992
[11] Wang J Z, Wang Z M, Wang Z G, Chen Y H and Yang Z 2000 *Phys. Rev.* B **61** 15614
[12] Keller O 1996 *Phys. Rep.* **268** 85–262
[13] Greffet J-J and Carminatti R 1997 *Prog. Surf. Sci.* **56** 133–237
[14] Keller O and Garm T 1994 *Phys. Scr.* T **54** 115–8
[15] Keller O and Garm T 1995 *Phys. Rev.* B **52** 4670
[16] Budkova N and Lozovski V 2000 *Ukr. Fiz. Zh.* **45** 225–9
Budkova N and Lozovski V 2000 *Ukr. J. Phys.* **45** 225–9 (Engl. Transl.)
[17] Tretyak O, Lvov V and Barabanov O 2002 *Physical Basis of Spin Electronics* (Kyiv: University Press)
[18] Ziese M and Thortron M J (ed) 2001 *Spin Electronics* (Berlin: Springer)
[19] Kolehmainen J, Reimann S M, Koskinen M and Manninen M 2000 *Eur. J. Phys.* B **13** 731
[20] Burkard G, Engel H-A and Loss D 2000 *Fortschr. Phys.* **48** 965
[21] Toda Y, Shinomori S, Suzuki K and Arakawa Y 1998 *Solid-State Electron.* **42** 1083
[22] Keller O and Garm T 1996 *J. Opt. Soc. Am.* B **13** 2121–8
[23] Baryakhtar I, Demidenko Yu, Kriuchenko S and Lozovski V 1995 *Surf. Sci.* **323** 142
[24] Zhuravlev A, Lozovski V and Khudik B 1992 *Ukr. Fiz. Zh.* **37** 1151
[25] Lozovski V 2001 *Physica* E **9** 642
[26] Maradudin A and Mils D 1975 *Phys. Rev.* B **11** 1392
[27] Halonen V, Pietiläinen P and Charkraborty T 1996 *Europhys. Lett.* **33** 377
[28] Troiani F, Hohenester U and Milinary E 2001 *Phys. Status Solidi* b **224** 849